Piezo2, A Pressure Sensitive Channel Is Expressed in Select Neurons of the Mouse Brain: a Putative Mechanism for Synchronizing Neural Networks by Transducing Intracranial Pressure Pulses

Jigong wang
The University of Texas Medical Branch at Galveston
owen peter hamill (ohamill@utmb.edu)
University of Texas Medical branch

Research

Keywords: Piezo2, intracranial pressure, neocortex, hippocampus, mitral cells, neural network synchronization

Posted Date: June 29th, 2021

DOI: https://doi.org/10.21203/rs.3.rs-600027/v1

Abstract

Piezo2 expression in mouse brain was examined using an anti-PIEZO2 antibody (Ab) generated against a C-terminal fragment of the human PIEZO2 protein. As a positive control for Ab staining of mouse neurons, the Ab stained a majority of mouse dorsal root ganglion (DRG) neurons, consistent with recent in situ hybridization and single cell RNA sequencing studies of Piezo2 expression. As a negative control and test for specificity, the Ab failed to stain human erythrocytes, which selectively express PIEZO1. In brain slices isolated from the same mice as the DRG, the Ab displayed high selectivity in staining specific neuron types, including pyramidal neurons in the neocortex and hippocampus, Purkinje cells in the cerebellar cortex and mitral cells in the olfactory bulb. Given the demonstrated role of Piezo2 channels in peripheral neurons as a low-threshold pressure sensor (i.e., ≤ 5 mm Hg) critical for the regulation of breathing and blood pressure, its expression in select brain neurons has interesting implications. In particular, we hypothesize that Piezo2 provides select brain neurons with an intrinsic resonance enabling their entrainment by the normal intracranial pressure (ICP) pulses (~ 5 mm Hg) associated with breathing and cardiac cycles. This mechanism could serve to increase the robustness of respiration-entrained oscillations previously reported across widely distributed neuronal networks in both rodent and human brains. This idea of a “global brain rhythm” has previously been thought to arise from the effect of nasal airflow activating mechanosensitive neurons within the olfactory epithelium, which then synaptically entrain mitral cells within the olfactory bulb and through their projections, neural networks in other brain regions, including the hippocampus and neocortex. Our proposed, non-synaptic, intrinsic mechanism in which Piezo2 tracks the “metronome-like” ICP pulses would have the advantage that spatially separated brain networks could also be synchronized by a physical force that is rapidly transmitted throughout the brain.

Introduction

In 2006, it was reported [2] that the rat ortholog of a human gene covering KIAA0233 [3] was transcriptionally induced in cultured rat astrocytes treated with aggregates of beta-amyloid (Aβ) —a major component of senile plaques in Alzheimer’s disease (AD^+). The gene was designated *Mib* (i.e., Membrane protein induced by Aβ) and predicted to encode a large membrane protein of >2000 amino acids that included>23 transmembrane domains [2]. Moreover, in situ hybridization (ISH) studies of human AD^+ brains reported selective *hMIB* expression in activated astrocytes surrounding Aβ-plaques. Significantly, in normal brains (i.e., AD^-) *hMIB* expression appeared to be strictly limited to neurons [2]. These key findings indicated that *Mib* expression is subject to an on-off switch that is cell-type sensitive and regulated by the surrounding brain conditions. In healthy brains, the switch is turned on in neurons, where presumably MIB performs a yet-to-be identified “homeostatic” function(s) important for neuronal function and/or survival. On the other hand, in AD^+ brains, the switch is turned on in activated astrocytes, where MIB may take on a neuropathological role [2]. Since an over-expressed GFP-tagged Mib was localized to the endoplasmic reticulum (ER), it was suggested that Mib (also known as Fam38A) may

function to regulate protein transport and signaling in the ER [2], possibly involving integrin activation by Mib/Fam38A [4].

In 2010, a critical advance was made in the Mib story by the demonstration, using a siRNA knockdown screen, that *Mib/Fam38A* actually forms a pressure-activated channel and accordingly the membrane protein was re-designated Piezo1 [5]. Vertebrates express two Piezo family members, Piezo1 (Fam38A) and its paralog Piezo2 (Fam38B) that show differential expression in various mouse tissues including peripheral and central neural tissues [5]. Most notably, *Piezo2* is more highly expressed compared with *Piezo1* in mouse DRG neurons, whereas *Piezo1* and *Piezo2* are expressed in equally low, but still at quantifiable levels in mouse brain tissue [5], possibly indicating low expression in many brain cell types, or select expression in only specific brain neurons [2]. In the case of Piezo1, subsequent studies have confirmed Piezo1 expression in brain neurons as well as astrocytes [2, 6–11]. Most significantly, Blumenthal et al. [6] studying rat hippocampal neuron-astrocyte interactions, proposed that the Piezo1 channel in neurons is able to sense and transduce the surface nanoroughness of astrocytes into trophic signals that maintain neuronal survival. However, in AD^{+} brains with the progressive build-up of mechanically stiff senile plaques, there is a detrimental increase in brain tissue nanoroughness that is transduced by Piezo1 into anti-survival signaling [6, see 12 for review]. Interestingly, other stressful conditions also increase Piezo1 expression in astrocytes, including those occurring with normal aging, bacterial infection, brain ischemia or exposure to demyelinating agents. Furthermore, experimental over activation of Piezo1 channels using Yoda1, a Piezo1 specific agonist [13] directly disrupts normal neuronal function and/or survival [11, 14–16].

In the case of Piezo2, most studies have focused on Piezo2 expression in peripheral neurons and its key sensory roles in touch, proprioception, micturition and the regulation of breathing and blood pressure [5, 17–25]. However, it has also been demonstrated, using RT-PCR [26] and Western blotting [26] that Piezo2 is expressed in rat neocortical and hippocampal tissues, and this expression is increased in response to repetitive mechanical (i.e., blast) injury (26, 27). These findings raise the possibility that a rapid mechanical activation of Piezo2 caused by concussion or mild traumatic brain injury (TBI) contributes to the rapid and often reversible disruptions in brain functions including loss of consciousness and memory. Furthermore, the observed changes in Piezo2 expression caused by repetitive TBI may contribute to long-term neurodegenerative processes and disorders that have been associated with TBI [26–29].

The above measurements of Piezo2 gene/protein expression in brain tissue do not discriminate between expression in specific neurons and/or non-neuronal cell types (e.g., glial and vascular cells). Therefore, we have use immunohistochemistry (IHC) to investigate cell-type specific Piezo2 expression in mouse brain. In brief, we find that Piezo2 is expressed in pyramidal neurons of the neocortex (NC) and hippocampus (HC), Purkinje cells of the cerebellar cortex, and most intriguingly, mitral cell of the olfactory bulb (OB). We propose that the activation of the highly pressure sensitive Piezo2 cation channel by normal (<10 mm Hg) or abnormal (>25 mm Hg) intracranial pressures (ICP) may increase neural excitability thereby altering neural circuit activity and brain function. Furthermore, we hypothesize that Piezo2 may confer on key neurons an intrinsic membrane resonance [1] that acts to synchronize their firing with the recurring,

pulsatile changes in ICP associated with breathing and cardiac cycles. In particular, this resonance could serve to increase the robustness of respiration entrained neural network oscillations reported previously in the OB, HC and NC and proposed to be driven by either synaptic inputs from peripheral afferents in the nasal epithelium or efferent copy discharges from brain stem respiratory nuclei [30–32]

Note after our IHC study was completed [33] another study using two different commercially available anti-PIEZO2 antibodies, reported similar results including near pan expression of Piezo2 in rat DRG neurons and also Piezo2 expression in NC and HC neurons but not astrocytes [34]. Moreover, another recent study using single nucleus and bulk RNA deep sequencing has confirmed that *Piezo2* is a genetic marker for specific mitral cells within the mouse OB [35].

Methods

Isolation of mouse brains and dorsal root ganglia

All experimental protocols were approved by the Animal Care and Use Committee at the University Texas Medical Branch (UTMB) and are in accordance with the NIH Guide for the Care and Use of Laboratory Animals. Young adult (20–25 g, ~10 weeks old) male C57BL/6J (n =3) or GAD67-GFP (n = 3) mice (Jackson Laboratory, Bar Harbor, Maine, USA). No differences were noted in the Ab staining patterns of the brain and DRG from the two strains of mice. Mice were deeply anesthetized with 5% isoflurane in oxygen, then after exposing the pleural cavity, perfused through the left ventricle first with cold heparinized saline aorta and then with 4% paraformaldehyde in 0.1 M phosphate-buffered saline (PBS). Their DRG and brains were rapidly removed and stored in the same fixative overnight. Subsequently, the brains and DRG were dehydrated through an ethanol series/xylene, embedded in paraffin and 10 µm sagittal slices cut. Human red blood cells were collected in the fixative, pelleted, dehydrated, and embedded in paraffin for slicing.

Antibody generation

The anti-PIEZO2 Ab was custom generated by Proteintech (Chicago, Ill) against a peptide fragment overexpressed from a cloned fragment of the human PIEZO2 (pF1KE0043) that we purchased from Kazusa DNA Research Institute (Chiba, Japan). This vector is suitable for expression of tag-free proteins in *E. coli* cells as well as in vitro protein-expression systems driven by T7 RNA polymerase. The antigen (protein epitope signature tag (PrEST)) was a 188 amino acid peptide corresponding to amino acids 2440-2628 located at the C-terminus of the human PIEZO2 isoform (NP_071351.2), corresponding to amino acids 2512-2700 of the mouse Piezo2 isoform (NP_001034574.4). The plasmid insert was sequenced to assure that the correct PrEST sequence was cloned and the size of the resulting recombinant protein (including the specific PrEST) was checked to ensure that the correct antigen has been produced and purified. The rabbit Ab was affinity purified using an antigen bound column. To control for cross-reactivity, the affinity purified Ab are tested for sensitivity and specificity on protein arrays consisting of glass slides with spotted PrEST fragments, including Piezo1 and 2 fragments.

A primary aim in selecting the specific PIEZO2 PrEST was that it would generate an anti-PIEZO2 Ab with maximum binding affinity for the native mouse Piezo2 protein still embedded in the membrane (i.e., with its tertiary structure retained). In particular, we chose the C-terminal 188 amino acid peptide that encompasses part of the extracellular domain that contributes to Piezo2 pressure sensitivity [91, 92]. Another reason for this choice was that the PrEST would generate an Ab with a high specificity for the mouse Piezo2 protein rather than, or in addition to, its paralog, Piezo1. The human PIEZO2 PrEST did display relatively high amino acid identity (i.e., 84%, with 158 out of 188 residue identical) for the corresponding region (2512-2700) of the mouse Piezo2 isoform (NP_001034574.4) but relatively low identity (i.e., 34.6% with 65 out of 188 residue identity) with the corresponding region (3226-3414) of the mouse Piezo1 isoform (NP_001032375.1). Finally and ideally, the staining pattern by our Ab should be reproducible with a different and independently generated anti-PIEZO2 Ab using a different PrEST. The PrEST we chose, actually by coincidence, also encompasses the shorter C-terminal peptide (122 amino acids) of the corresponding to amino acids 2446-2568 of PIEZO2 used to generate the commercial anti-PIEZO2 Ab (Atlas antibodies, HPA015986)[4]. This Ab used by the Human Protein Atlas shows selective staining of neurons within the human neocortex, hippocampus and most notably Purkinje cells of the cerebellar cortex. Furthermore, based on the orthogonal consensus/validation between the HPA015986 Ab protein staining and GTex RNA sequencing data of the human brain, HPA has assigned the Ab an "Approved" reliability score[5]. This designation reflects a 2021 revision in the HPA database (Dr. Katona, HPA Tissue Atlas team

Uppsala University, personal communication). Finally, a recent IHC study used two independently generated, and genetically validated anti-PIEZO2 Abs recognizing different Piezo2 epitopes (Table 1), that show similar pan staining of DRG neurons as well as staining neurons in the HC and NC [34]

Footnote 4: https://www.atlasantibodies.com/api/print_datasheet/HPA015986.pdf

Footnote 5: https://www.proteinatlas.org/ENSG00000154864-PIEZO2/tissue

Detecting Ab immunoreactivity

The Piezo2 immuno-reactivity was detected using the anti-PIEZO2 Ab at a 1:600 dilution for 60 minutes. The brain and DRG tissues were processed using the Dako Autostainer. The secondary Ab used was biotinylated goat anti-rabbit IgG (Vector Labs, Burlington, CA, #BA-1000) at 1:200 for 30 minutes followed by Dako LSAB2 streptavidin-HRP (#SA-5704) for 30 minutes. Slides were developed with Dako DAB chromagen (#K3468) for 5 minutes and counterstained with Harris Hematoxylin for one minute. Imaging was carried out under bright field Olympus Bx51 microscope with Olympus DP imaging software. DRG and brain slices were viewed and Ab stained cells counted in magnified (40x or 60x objectives) brain sections.

Results

The Anti-PIEZO2 Ab stains a majority of neurons in the mouse DRG

For this IHC study, we used a custom-generated antibody raised against a C-terminal peptide fragment (2440–2628) of the human PIEZO2 (see methods). As a positive control for staining of Piezo2 in mouse neurons, we used mouse DRG sensory neurons, where Piezo2 was first identified [5]. As indicated in Figs. 1A, B, the Ab stained the large majority mouse DRG neurons (≥ 90%) including the smallest (~ 10 μm) largest (~ 50 μm) diameter neurons. This almost pan expression of Piezo2 is in line with more recent ISH [21, 36], scRNA-seq [20, 37] and IHC studies [34]. Figures 1C, D demonstrated the lack of nonspecific staining by the secondary antibody using same IHC protocol but in the absence of the anti-Piezo2 Ab. The numerous small blue structures (i.e., stained by the nuclear stain hematoxylin) around the perimeter of each neuron (Figs. 1B-C) represent the nuclei of satellite glia cells (SGCs) that ensheath the neurons with very thin cytoplasmic processes. Although the SGCs appeared to show no Ab staining, this could be an issue of detection rather than a lack of Piezo2 expression [34]. On the other hand, previous ISH studies also indicated a lack of *Piezo2* gene expression in SGCs [17, 36], which was in contrast to the strong *Piezo1* expression, particularly evident in SCG nuclei [36]. Because Piezo1 is also expressed in rodent DRG neurons [34, 36, 38] as well as in brain neurons [2], we further tested and confirmed our anti-PIEZO2 Ab specificity by its lack of cross reactivity with PIEZO1, which is selectively expressed in human red blood cells [39] (data not shown).

The Ab selectively stains pyramidal neurons in the mouse neocortex and hippocampus

Using brain slices from the same mice that the DRG were isolated and following identical IHC protocols, we examined the expression of Piezo2 in different brain regions, specifically focusing on regions where neurons classes are easily identifiable based on their morphology and characteristic layered arrangement. In particular, the Ab stained many cells in the grey matter of the neocortex, most notably cells spanning across the layer V-VI boundary (Fig. 2A). Examination at high magnification indicated that the stained neurons were mostly pyramidal-like, according to their triangular shaped cell body and unitary (apical) dendrite oriented perpendicular to the cortical layers and directed towards the pia (Fig. 2B). In contrast, we saw no evidence of staining of multipolar cells that may have represented stellate interneurons or astrocytes.

In the case of the hippocampus, the Ab showed selectivity in staining neurons in specific regions of the hippocampus. Figure 3A shows at low magnification the different regions (dentate gyrus, CA1-4) and Fig. 3B shows a more magnified CA3 region in which ~ 30% of the neurons (i.e., 10/35) showed clear staining. Figure 4 shows individual regions of the hippocampus from the same mouse brain slice at higher magnification indicating relatively stronger Ab staining of neurons in the CA3 and CA2 regions. For example, in the dentate gyrus (DG) only ~ 1% of cells (i.e., 16/1149) showed distinct Ab staining ((Fig. 4A-C) and these were mostly spindle shaped cells located in the sub-granular layer, possibly reflecting interneurons. Similarly, in the hilius/C4 regions, only ~ 3% of neurons (i.e., 2/72) showed staining

(Fig. 4D). In comparison, in the CA3 and CA2 regions, ~ 36% (i.e., 50/140) and 21% (i.e., 15/71) of neurons, respectively, showed Ab staining (Figs, 4E-H) compared with only ~ 8% (23/305) in the CA1 region (see Figs. 4I-L). Most of the neurons stained were pyramidal neurons as judged by their location and dendritic tree. A similar pattern of higher proportional staining of neurons in the CA3-CA2 regions (i.e., 150/514) compared with the other hippocampal regions (i.e., 85/2850) was seen in analysis of two different mouse brains.

Our results for the mouse NC and HC can be compared with PIEZO2 expression reported by the Human Protein Atlas (HPA) using a different Ab generated against a shorter PIEZO2 peptide (C-termini 2446–2568). In the HPA case, PIEZO2 was also seen to be expressed in neurons but not astrocytes of the human NC and HC and the specific Ab was orthogonally validated by *PIEZO2* gene expression in human NC and HC tissues measured by RNA-sequencing [40, 41][1]. Furthermore, and as already noted, a recent IHC study of the rat brain using two different commercial anti-PIEZO2 Abs raised against peptides in different regions of PIEZO2 (Table 1) also indicate Piezo2 expression in NC and HC neurons but not in astrocytes [34].

Footnote 1: https://www.proteinatlas.org/ENSG00000154864-PIEZO2/tissue

The Ab stains Purkinje cells but not granule cells in the cerebellar cortex

As indicated in Fig. 5, the Ab selectively stained Purkinje cells (PC) in the cerebellar cortex including their relatively large cell bodies and the branching dendrites that extend into the molecular cell layer (Fig. 5B). In marked contrast, the granule cells (GC) that form the granular layer showed no evidence of staining. This all-or-none selectivity in staining PC vs GC highlights the selectivity in Piezo2 expression given a PC: GC ratio of 1:3000 in the cerebellar cortex [42]. However, as indicated Fig. 5A (i.e., yellow circle) some neurons embedded within the cerebellar white matter (arbor vitae) and possibly representing projection neurons within a deep cerebellar nucleus showed Ab staining. Similar selective staining of PC in the human cerebellar cortex have been previously reported by the HPA using a different anti-PIEZO Ab [40][2]

Footnote 2: https://www.proteinatlas.org/ENSG00000154864-PIEZO2/tissue/cerebellum

The Ab selectively stains mitral cells in the olfactory bulb

Figure 6A shows a low magnification image of the mouse OB and indicates Ab staining of the OB neuropil with the circular glomeruli delineated by the hematoxylin stain. Figures 6B-D show progressively magnified images of the same OB indicating the strongest staining was of the mitral cells that form a distinct boundary cell layer separating the plexiform from the granular cell layers. The staining of the neuropil in the external plexiform layer presumably represents stained mitral cell dendrites that project to the glomeruli where they receive synaptic inputs from primary olfactory neurons (PONs). Tufted cells located in the external plexiform layer, which also receive synapses from PONs, did not appear stained. Also as indicated in Fig. 6D, the most abundant cells of the OB, the granule cells were unstained.

The expression of Piezo2 in the OB mitral cells was unanticipated, especially given the well-recognized role of mitral cells in processing primary olfactory sensory inputs, without any requirement for intrinsic mechanosensitivity. However, as already noted, a recent study using single nucleus and bulk RNA deep sequencing has confirmed that *Piezo2* is a genetic marker of specific mitral cells within the mouse OB [35].

Discussion

The results of this IHC study indicate that the Piezo2 protein is expressed in pyramidal neurons of the NC and HC, Purkinje cells of the cerebellar cortex and mitral cells of the OB. These results are consistent with earlier and more recent studies of Piezo2 expression rodent and human brains [26, 27, 34, 35, 40, 41]. Although Piezo2 is well established as a pressure sensitive channel in peripheral neurons [5, 17-25] further functional studies, using patch clamp [43] and/or single cell Ca^{2+} imaging [44] are required to confirm that Piezo2 is functionally active in these different neuron types. Interestingly, the first patch clamp study demonstrating single pressure-activated single channel currents in NC and HC pyramidal neurons in mouse brain slices, indicated a low frequency channel activity in the absence of applied pressure that increased in frequency with increasing steady state pressure [43]. Furthermore, recording from a CA3 pyramidal neuron (see Figure 8 of ref. 43) demonstrated that relatively brief (~ 1 s) negative pressure pulses of >25 mm Hg were able to stimulate repetitive firing of action potentials at increasingly higher frequencies (e.g., 3 Hz with a 27 mm Hg pulse and 24 Hz with a 31 mm Hg pulse). In the future, it will be important to extend these studies to positive pressure pulses which have been reported to selectively activate Piezo2 channels [e.g., see 45].

It is also worth considering the nature (e.g., amplitude and time course) of the exogenous and endogenous pressure that neurons might experience within the brain that might be capable of activating Piezo2 channels. The finding that large exogenous pressures, simulating blast forces, alter Piezo2 channel expression in the NC and HC [26, 27], particularly in response to repetitive blasts, indicates the potential for a neuropathological role of Piezo2 in traumatic brain injury (TBI). Moreover, one might expect that abnormal activation of Piezo2 in these brain regions could contribute to the acute and often reversible deficits in motor, sensory and cognitive functions associated with concussion and mild TBI. However, TBI is just one of several neuropathological conditions, including hydrocephalus, cerebral hemorrhage and brain tumors, known to elevate the normally low (< 10 mm Hg) baseline intracranial pressure (ICP) to higher levels (> 25 mm Hg), all with serious clinical consequences [46-49]. Given positive pressures pulses as low as ≤ 5 mm Hg can activate Piezo2 channels [45], it would not be surprising that pressures 5-fold higher would induce abnormal Piezo2 activities and contribute to deficits in brain function. A special case is normal pressure hydrocephalus (NPH) in which enlarging ventricles compress the brain parenchyma [50]. Interestingly, the dementia associated the NPH is often misdiagnosed as Alzheimer's disease (AD), but can be distinguished by ventriculoperitoneal shunts that reduce ICP, and often rapidly reverses this form of dementia [50].

In terms of evolution and natural selection, there would seem little selective advantage for brain neurons to express Piezo2, especially if the channel only functions in a neuropathological role, with no benefit for improved normal brain performance. Therefore, a more relevant and interesting question is whether smaller changes in ICP (≤ 10 mm Hg) that occur in the healthy brain might also produce changes in Piezo2 activity and thereby somehow enhance normal brain function. Although ICP in healthy subjects is maintained at low baseline values of 0-10 mm Hg [46, 49] ICP also undergoes metronomic-like, pulsatile changes involving rapid (~200 ms) pulses with each heartbeat [46-48], as well as much slower (5-10 s) pulses associated with breathing [51-53]. Moreover, specific volitional breathing practices —involving slow inspiration/expiration cycles and/or diaphragmatic vs thoracic breathing — performed to improve attention or reduce stress/anxiety, cause even larger pulsatile changes in ICP [53]. This raises the intriguing possibility that the presence of Piezo2 might allow specific neurons to transduce these pulsatile ICP changes, thereby entraining the rhythmic neural network oscillations previously measured with EEG and shown to underlie specific brain/behavioral states [54-56]. In this case, it may be that the pulsatile fluctuations in ICP started out as epiphenomena [1] representing the unavoidable cerebral responses to breathing and cardiac rhythms. However, over time selective pressure would tend to favor Piezo2 expression, if that conferred on neurons a new mechanism for synchronizing neural network communication, especially within the much larger brains of humans.

Direct experimental evidence for the actual idea that breathing can induce entrainment of neural networks goes back 80 years with the discovery by Edgar Adrian in 1942 that nasal breathing in rodents causes rhythmic firing of mitral neurons within the OB, as well as neurons within the piriform cortex [57]. Many subsequent studies have verified and extended his discovery, showing that nasal breathing, not only entrains OB oscillations at the rodent's breathing frequency (0.5- 5 Hz), but also modulates the amplitude of higher frequency oscillations (80 -120 Hz) in the OB as well as other downstream brain regions including the HC and NC [30-32] . Furthermore, these neural network oscillations have been associated with specific changes in rodent behaviors including whisking, memory formation and emotional (fear) responses [58-67]. Perhaps most significantly, many of the observations related to respiration-locked oscillations seen in rodents, have now been confirmed in humans, using either intracranial EEG recording from epileptic patients or high density EEG recording from healthy subjects [55, 56, 68, 69].

Three different, non-mutually exclusive mechanisms may explain respiration entrained neural network oscillations [30-32, 70-72]. The first mechanism, referred to as olfactory re-afferent discharge (ORD) proposes that nasal airflow during nasal breathing activates mechanosensitive primary olfactory neurons (PON) within the nasal epithelium turn activating via their direct synaptic connections, mitral cells within the OB [72, see Fig. 7]. In this mechanism, the OB acts as a "global clock" for other brain regions, synchronizing via its synaptic connections, neural networks across widespread brain regions, including the HC and NC [31, 32]. Evidence supporting this mechanism, is that tracheotomy or ablation of the nasal epithelium (or removal of the OB) in rodents, reduces the synchronized activity in the OB and/or in downstream brain regions [57, 58, 73, 74]. Moreover, in both humans and rodents, air pressure pulses delivered to the nostrils can restore and/or alter the oscillation frequency [63, 68].

The second mechanism referred to as “respiratory corollary discharge” (RCD) depends upon efferent copy discharges from neurons in the brain stem nuclei that regulate breathing [75-77, Fig. 7]. Support for this mechanism includes the finding that although tracheotomy or ablation of the nasal epithelium reduces the neural oscillations in rodents, they do not completely block them [58, 77]. Moreover, in humans the oscillations persist during mouth breathing and therefore in the absence of any nasal airflow) [69, 77]. Further evidence for the RCD mechanism is that neurons in the brain stem respiratory nuclei form connections with neurons in the locus coeruleus that via their projections may alter activity in widely spaced neural networks throughout the brain [76].

The third mechanism, and the least investigated, we refer to as intrinsic resonance discharge (IRD). In this case, it is the intrinsic properties of the neural networks involving either intrinsic neuronal membrane properties or synaptic micro-circuitry, which dictates that they fire or resonate at a frequency close to the respiratory frequency [56]. The evidence also for the IRD mechanism is again that respiration-entrained oscillations are retained during mouth breathing or in the absence of nasal airflow or functional PONs, [58, 69, 77]. Moreover, IRD may in part account for a somewhat puzzling feature of the ORD mechanism, which relates to the mechanosensitivity of the odor sensitive GPCR in the PONs. Evidence indicates that their mechanosensitivity depends upon a second messenger pathway, and consequently display long latencies of ~300 ms in response to pressure pulses [72]. Furthermore, because of GPCR adaptation, their maximum frequency response to repetitive pressure pulse stimuli has been measured at only 0.5 Hz [72], which is significantly slower than the rodent’s normal breathing frequency and entrainment frequency induced in the mitral cells of the OB (2-6 Hz). Although the convergence of many PON inputs to the mitral cells may still generate rhythmic activity that follows respiration, even when only a fraction of the PONs responding with each respiratory cycle [see 72], an alternative or reinforcing mechanism could be that the mitral cells themselves possess an intrinsic resonance to the breathing cycle. Specifically, we hypothesize that Piezo2 in mitral cells, as well as neurons in the NC and HC, confer an intrinsic resonance that further reinforces their entrainment by the breathing via their transduction of pulsatile ICP changes (Fig. 7). Because stretch activated channels, including Piezo channels, are characterized by their fast gating [78] and ability to accurately track relative high frequency (e.g., ³ 5 Hz) pressure pulses [79, 80] they could confer resonance for breathing-associated, as well as the even higher frequency cardiac-associated, ICP pulses [46-48, 81-83]. Moreover, the expression of Piezo2 in cerebellar PC may also explain the sniffing dependent activation of the human cerebellum [84] and the highly correlated slow (~ 1 Hz) oscillations seen between mouse PCs [85].

An intrinsic Piezo2/ICP resonance mechanism may also developed a more important role for human breathing-induced entrainment because of additional selective pressures. In particular, in humans nasal breathing is not obligatory as in rodents. Also in humans, olfaction has become a relatively unimportant sensory function, adding only little advantage for survival, which is unlike in rodents where olfaction, sniffing and whisking are tightly linked and critical for their normal behavior and survival. Moreover, humans are the only species capable of volitionally switching breathing patterns (e.g., to forced inspiration/expiration cycles) in order to promote changes in mood, cognition and emotions. Humans are also unique in that they consciously modulate through their breathing, both their heartbeat and emotions

[81, 82]. Interestingly, on this point a study of single unit recording from epileptic patients indicated a higher proportion of hippocampal and amygdala neurons show entrainment with the cardiac cycle compared with the respiratory cycle [83].

Regardless of the exact mechanism, a key issue for all mechanisms is their reliability and degree of synchronization that they can induce within widely separated neural networks. This synchronization has special implications for the unity of experience, as it relates to perception, motor control and memory retrieval, especially in the much larger human brain. In the case of the first two mechanisms, the overall synchronization will depend upon signaling delays within multi-synaptic, axonal transmission pathways. In comparison, the Piezo2/ICP pulse dependent IRD mechanism will only be rate limited by the speed of ICP pulse transmission throughout the brain, powered by the perennial actions of the respiratory and cardiac pumps. In the ideal case when Pascal's law applies, namely a rigid, fluid-filled and closed container, a pressure pulse will spread throughout the container almost instantaneously at the speed of sound (i.e., ~1500 m/s) [46]. However, this may represent an upper estimate since the brain contained within the skull is actually a semi-closed system that involves cerebral venous outflow as well as arterial inflow [45-47]. Plus, CSF and blood tend to circulate between the brain and spinal cord, particularly during inspiration and expiration [51-53]. In addition, the brain parenchyma, ventricles, and vasculature are themselves compliant rather than rigid, which will also tend to dissipate and slow the spread of ICP changes. In one notable study [86], aimed at measuring ICP transmission in the human brain, two ICP sensors, placed 5 cm apart in the lateral ventricle and brain parenchyma, measured a phase shift of 10 ms [86]. This would predict a pulse velocity of only 5 m/s. (i.e., which compares with a predicted 50 ms phase shift for a velocity of 1,500 m/s). However, there are two caveats regarding this lower estimate. First, the ICP pulse does not have a single origin but arises throughout the arterial tree [46]. Second, the pressure pulsations may occur within the dense microvascular embedded in the parenchyma so that no individual neuron is more than 100 mm from a pulsating vessel [87]. Both effects would tend to minimize delays and thereby synchronize the ICP pulse transmission to all neurons within neural networks throughout the brain.

Limitations and future studies

The results of any IHC study are dependent on the specificity/selectivity of the Ab as determined by various Ab validation criteria including genetic, orthogonal and independently generated Abs [40][3]. Although now four independently generated anti-PIEZO2 Abs including ours, raised against different regions of the PIEZO2 protein [26, 27, 34, 40 Table1] indicate Piezo2 expression in the rodent and human brain. Nevertheless, further verification with techniques independent of antibodies are required. For example, by the development and use of highly sensitive GFP- tagged *Piezo2* transgenic mice [e.g., 88, GENSAT]. Given *Piezo1* is also expressed in rodent and human brain neurons [2] and that both Piezo1 and Piezo2 are essential for pressure sensation in peripheral baroreceptors [24] it will also be important to establish the expression patterns and the specific roles of both Piezo channels in the different brain neurons (i.e., by using also a combination GFP-tagged *Piezo* transgenic mouse). The functional expression of pressure-activated channels in the specific neuron types in mouse brain slices and ideally

in situ in the brains of living/breathing animals needs to be verified and these studies should be combined with conditional Piezo knock out mice in order to establish the channel's molecular identity.

Footnote 3: https://www.proteinatlas.org/about/assays+annotation#ihk

Perhaps the biggest challenge in terms of testing the intrinsic resonance hypothesis will be to demonstrate that Piezo channels, actually participate in the entrainment of neural network oscillations. One possible approach may be to use the conditional Piezo knock out mice and compare respiratory entrained neural network oscillations with those reported previously for wild type mice [30-32, 59-61]. It would also be very interesting to study human patients that show a specific loss of Piezo2 function [89], to determine how their measured EEG and behavioral responses to specific breathing protocols, compare with reported responses of normal human subjects [54-56, 68, 69].

Finally, we would like to end where we began with a more compete version of the quote from Hutcheson and Yaron [1]. *"A question therefore arises: are resonances used by neurons or are they simply epiphenomena?" A broad answer to this question is that, in nature, epiphenomena seldom remain epiphenomena for long; they are the raw material for evolutionary advances. It would be surprising to find that the brain has not found a use for a set of mechanisms capable of tuning neurons to specific frequencies, particularly in light of the prevalence of robust brain rhythms."* Here, Hutcheson and Yarom are referring to, at the time, the relatively unexplored role of the various EEG recorded electrical brain rhythms [90]. However, it may be the metronomic-like and perennial ICP pulses, transduced by pressure sensitive channels, prove even more pivotal in tuning and synchronizing the brain to the fundamental frequencies of life.

Declarations

Ethics approval

All experimental protocols were approved by the Animal Care and Use Committee at the University Texas Medical Branch (UTMB) and are in accordance with the NIH Guide for the Care and Use of Laboratory Animals

Consent for publication

Not applicable

Availability of data and materials

Please contact authors for data requests.

Funding

Funding for JW was provided by an NIH Grant RO1 NS03168 to Dr. Jin Mo Chung

Competing interests

“The authors declare that they have no competing interests.”

Authors’ contribution

JW surgically isolated and prepared the mouse brains and DRG. OH conceived the study, analyzed and interpreted the IHC experiments and wrote the manuscript. All authors read and approved the final manuscript.

Acknowledgments

We thank Dr. Jin Mo Chung for providing financial support and Drs. Daniel Jupiter, Andrzej Kudlicki and Thomas Green for helpful discussions. We also appreciate the assistance from the UTMB Pathology core facility, and in particular, Kerry Graves for preparing the brains and DRG slices for IHC. We also thank Kenneth Escobar for providing the microscopy facilities

References

1. Hutcheon B, Yarom Y. Resonance, oscillation and the intrinsic frequency preferences of neurons. Trends Neurosci. 2000; 23: 216-222.
2. Satoh K, Hata M, Takahara S, Tsuzaki H, Yokota H, Akatsu, H, et al. A novel membrane protein, encoded by the gene covering KIAA0233, is transcriptionally induced in senile plaque-associated astrocytes. Brain Res. 2006; 1108: 19–27.
3. Nagase T, Seki N, Ishikawa K, Ohira M, Kawarabayasi Y, Ohara O, et al. Prediction of the coding sequences of unidentified human genes: VI. The coding sequences of 80 new genes (KIAA0201-KIAA0280) deduced by analysis of cDNA clones from cell line KG-1 and brain. DNA Res. 1996; 3: 321–329.
4. McHugh BJ, Buttery R, Lad Y, Banks S, Haslett C. Integrin activation by Fam38A uses a novel mechanism of R-Ras targeting to the endoplasmic reticulum. J. Cell Sci. 2010; 123: 51–61.
5. Coste B, Mathur J, Schmidt M, Taryn J, Earley TJ, Ranade S, et al. Piezo1 and Piezo2 are essential components of distinct mechanically activated cation channels. Science. 2010; 330: 55–60.
6. Blumenthal NR, Hermanson O, Heimrich B, Prasad Shastri V. Stochastic nanoroughness modulates neuron–astrocyte interactions and function via mechanosensing cation channels. Proc Nat Acad Sci USA. 2014; 111:16124–16129.
7. Pathak MM, Nourse JL, Tran T, Hwe J, Arulmoli J, Le DT, et al Stretch-activated ion channel Piezo1 directs lineage choice in human neural stem cells. Proc Natl Acad Sci U S A. 2014: 111; 16148-16153.
8. Zeisel A, Muñoz-Manchado AB, Codeluppi S, Lönnerberg P, La Manno G, Juréus A, et al. Brain structure. Cell types in the mouse cortex and hippocampus revealed by single-cell RNA-seq. Science.

2015; 347:1138-1142.

9. Habib N, Li Y, Heidenreich M, Swiech L, Avraham-Davidi I, Trombetta JJ, et al. Div-Seq: Single-nucleus RNA-Seq reveals dynamics of rare adult newborn neurons. Science. 2016; 353: 925-928.
10. Wang YY, Zhang H, Ma T, Lu Y, Xie HY, Wang W, et al. Piezo1 mediates neuron oxygen-glucose deprivation/reoxygenation injury via Ca^{2+}/calpain signaling. Biochem Biophys Res Commun. 2019; 513:147-153.
11. Velasco-Estevez M, Mampay M, Boutin H, Chaney A, Warn P, Sharp A, et al. Infection Augments Expression of Mechanosensing Piezo1 Channels in Amyloid Plaque-Reactive Astrocytes. Front Aging Neurosci. 2018; 10: 332. doi: 10.3389/fnagi.2018.00332
12. Hall CM, Moeendarbary E, Sheridan GK. Mechanobiology of the brain in ageing and Alzheimer's disease. Eur J Neurosci. 2020; 1-28. doi: 10.1111/ejn.14766. Epub ahead of print. PMID: 32356339.
13. Syeda R, Xu J, Dubin AE, Coste B, Mathur J, Huynh T, et al. Chemical activation of the mechanotransduction channel Piezo1. eLife. 2015; 4: e07369.
14. Velasco-Estevez M, Gadalla KKE, Liñan-Barba N, Cobb S, Dev KK, Sheridan GK. Inhibition of Piezo1 attenuates demyelination in the central nervous system. Glia. 2020; 68: 356-375.
15. Velasco-Estevez M, Rolle SO, Mampay M, Dev KK, Sheridan GK. Piezo1 regulates calcium oscillations and cytokine release from astrocytes. Glia. 2019; 68:145-160.
16. Luo H, Liu H, Bian W, Chen B, Yang D, Yang M. Yoda1 Activates Piezo1 in Vitro to Simulate the Upregulation of Piezo1 in the Infected Brain: Piezo1 Participates in the Immune Activation of Microglia.- 2021 - researchsquare.com. DOI: https://doi.org/10.21203/rs.3.rs-274391/v1
17. Ranade SS, Woo SH, Dubin AE, Moshourab RA, Wetzel C, Petrus M, et al. Piezo2 is the major transducer of mechanical forces for touch sensation in mice. Nature. 2014; 516: 121-125.
18. Woo S H, Lukacs V, de Nooij JC, Zaytseva D, Criddle CR, Francisco A, et al. Piezo2 is the principal mechanotransduction channel for proprioception. Nat. Neurosci. 2015; 18: 1756-1762.
19. Woo SH, Ranade S, Weyer AD, Dubin AE, Baba Y, Qiu Z, et al. Piezo2 is required for Merkel-cell mechanotransduction. Nature. 2014; 509: 622-626.
20. Usoskin D, Furlan A, Islam S, Abdo H, Lönnerberg P, Lou D, et al. Unbiased classification of sensory neuron types by large-scale single-cell RNA sequencing. Nat Neuro. 2015; 18: 145–153.
21. Zhang M, Wang Y, Geng J, Zhou S, Xiao B. Mechanically Activated Piezo Channels Mediate Touch and Suppress Acute Mechanical Pain Response in Mice. Cell Rep. 2019; 26: 1419-1431.
22. Florez-Paz D, Bali KK, Kuner R, Gomis AA. Critical role for Piezo2 channels in the mechanotransduction of mouse proprioceptive neurons. Sci. Rep. 2016; 6: 25923.
23. Nonomura K, Woo SH, Chang RB, Gillich A, Qiu Z, Francisco AG, et al. Piezo2 senses airway stretch and mediates lung inflation-induced apnoea. Nature. 2017; 541:176-181.
24. Zeng WZ, Marshall KL, Min S, Daou I, Chapleau MW, Abboud FM, et al. PIEZOs mediate neuronal sensing of blood pressure and the baroreceptor reflex. Science. 2018; 362: 464–467.

25. Marshall KL, Saade D, Ghitani N, Coombs AM, Szczot M, Keller J, et al. PIEZO2 in sensory neurons and urothelial cells coordinates urination. Nature. 2020; 588:290-295.
26. Sajja VSSS, Ereifej ES, VandeVord PJ. Hippocampal vulnerability and subacute response following varied blast magnitudes. Neurosci Lett. 2014; 570: 33–37.
27. Heyburn L, Abutarboush R, Goodrich S, Urioste R, Batuure A, Statz J. et al. Repeated Low-Level Blast Overpressure Leads to Endovascular Disruption and Alterations in TDP-43 and Piezo2 in a Rat Model of Blast TBI. Front Neurol. 2019; 766: doi: 10.3389/fneur.2019.00766.
28. Mortimer JA, van Duijn CM, Chandra V, et al. Head trauma as a risk factor for Alzheimer's disease: a collaborative re-analysis of case-control studies. EURODEM Risk Factors Research Group. Int J Epidemiol. 1991; 20: S28–35.
29. Nogueira ML, Epelbaum S, Steyaert JM, Dubois B, Schwartz L. Mechanical stress models of AD pathology. Alzheimer's & Dementia. 2016; 12: 324-333.
30. Fontanini A, Bower JM. Slow-waves in the olfactory system: an olfactory perspective on cortical rhythms. Trends Neurosci. 2006; 29: 429-437.
31. Heck DH, McAfee SS, Liu Y, Babajani-Feremi A, Rezaie R, Freeman WJ, et al. Breathing as a Fundamental Rhythm of Brain Function. Front Neural Circuits. 2017; 10:115.
32. Tort ABL, Brankačk J, Draguhn A. Respiration-Entrained Brain Rhythms Are Global but Often Overlooked. Trends Neurosci. 2018; 41: 186-197.
33. Wang J, Hamill OP. Piezo2, a pressure sensitive channel is expressed in select neurons of the mouse brain: a putative mechanism for synchronizing neural networks by transducing intracranial pressure pulses. bioRxiv 2020.03.24.006452; doi: https://doi.org/10.1101/2020.03.24.006452
34. Shin SM, Moehring F, Itson-Zoske B, Fan F, Stucky CL, Hogan QH, et al. Piezo2 mechanosensitive ion channel is located to sensory neurons and non-neuronal cells in rat peripheral sensory pathway: implications in pain. bioRxiv 2021.01.20.427483; doi: https://doi.org/10.1101/2021.01.20.427483
35. Zeppilli S, Ackels T, Attey R, Klimpert N, Ritola KD, Boeing S, Crombach A, Schaefer AT, Fleischmann A Molecular characterization of projection neuron subtypes in the mouse olfactory bulb. bioRxiv 2020.11.30.405571; doi: https://doi.org/10.1101/2020.11.30.405571
36. Wang J, La JH, Hamill OP. PIEZO1 is selectively expressed in small diameter mouse DRG neurons distinct from neurons strongly expressing TRPV1. Front. Mol. Neurosci. 2019; 12: 178.
37. Sharma N, Flaherty K, Lezgiyeva K, Wagner DE, Klein AM, Ginty DD. The emergence of transcriptional identity in somatosensory neurons. Nature. 2020; 577: 392–398.
38. Roh J, Hwang SM, Lee SH, Lee K, Kim YH, Park CK. Functional Expression of Piezo1 in Dorsal Root Ganglion (DRG) Neurons. Int J Mol Sci. 2020; 21: 3834. doi: 10.3390/ijms21113834. PMID: 32481599
39. Ma S, Cahalan S, LaMonte G, Grubaugh ND, Zeng W, Murth SE, et al. Common PIEZO1 allele in african populations causes RBC dehydration and attenuates plasmodium infection. Cell. 2018; 173: 443–455.

40. Uhlén M, Fagerberg L, Hallström BM, Lindskog C, Oksvold P, Mardinoglu A, et al., Tissue-based map of the human proteome. Science. 2015; 347: 1260419.
41. GTEx Consortium. The Genotype-Tissue Expression (GTEx) pilot analysis: multi-tissue gene regulation in humans. Science. 2015; 348: 648–660
42. Lange, W. Cell number and cell density in the cerebellar cortex of man and some other mammals. Cell Tissue Res. 1975; 157:115-124.
43. Nikolaev YA, Dosen PJ, Laver DR, Van Helden DF, Hamill OP. Single mechanically-gated cation channel currents can trigger action potentials in neocortical and hippocampal pyramidal neurons. Brain Res. 2015; 1608: 1-13.
44. Gaub BM, Kasuba KC, Mace E, Strittmatter T, Laskowski PR, Geissler SA. et al. Neurons differentiate magnitude and location of mechanical stimuli. Proc Natl Acad Sci USA. 2020; 117: 848-856.
45. Shin KC, Park HJ, Kim JG, Lee IH, Cho H, Park C, et al. The Piezo2 ion channel is mechanically-activated by low-threshold positive pressure. Sci Rep. 2019; 9: 6446.
46. Czosnyka M, Pickard J. Monitoring and interpretation of intracranial pressure. J Neurol Neurosurg Psychiatry. 2004; 75: 813–821.
47. Wagshul ME, Eide PK, Madsen JR. The pulsating brain: A review of experimental and clinical studies of intracranial pulsatility. Fluids Barriers CNS. 2011; 8:5.
48. Greitz D, Wirestam R, Franc A, Nordell B, Thomsen C, Ståhlberg F. Pulsatile brain movement and associated hydrodynamics studied by magnetic resonance phase imaging. The Monro-Kellie doctrine revisited. Neuroradiol. 1992; 34: 370-80.
49. Andresen M, Hadi A, Petersen LG, Juhler M. Effect of postural changes on ICP in healthy and ill subjects. Acta Neurochir (Wien). 2015; 157:109-113.
50. Griffa A, Van De Ville D, Herrmann FR, Allali G. Neural circuits of idiopathic Normal Pressure Hydrocephalus: A perspective review of brain connectivity and symptoms meta-analysis. Neurosci Biobehav Rev. 2020; 112:452-471.
51. Dreha-Kulaczewski S, Joseph AA, Merboldt KD, Ludwig HC, Gärtner J, Frahm J. Inspiration is the major regulator of human CSF flow. J Neurosci. 2015; 35: 2485-2491.
52. Dreha-Kulaczewski S, Joseph AA, Merboldt KD, Ludwig HC, Gärtner J, Frahm J. Identification of the Upward Movement of Human CSF In Vivo and its Relation to the Brain Venous System. J Neurosci. 2017; 37: 2395-2402.
53. Aktas G, Kollmeier JM, Joseph AA, Merboldt KD, Ludwig HC, Gärtner J, et al. Spinal CSF flow in response to forced thoracic and abdominal respiration. Fluids Barriers CNS. 2019; 16: 10. doi: 10.1186/s12987-019-0130-0.
54. Moore, A., Gruber, T., Derose, J., and Malinowski P. Regular, brief mindfulness meditation practice improves electrophysiological markers of attentional control. Front Hum Neurosci. 2012: 6; 18. doi: 10.3389/fnhum.2012.00018. eCollection 2012.

55. Zelano C, Jiang H, Zhou G, Arora N, Schuele S, Rosenow J, et al., Nasal Respiration Entrains Human Limbic Oscillations and Modulates Cognitive Function. J. Neurosci. 2016; 36: 12448-12467.
56. Herrero JL, Khuvis S, Yeagle E, Cerf M, and Mehta AD. Breathing above the brain stem: volitional control and attentional modulation in humans. J Neurophysiol. 2018; 119:145–159.
57. Adrian ED. Olfactory reactions in the brain of the hedgehog. J Physiol. 1942; 100: 459-473.
58. Fontanini A, Spano PF, Bower JM. Ketamine-Xylazine-Induced Slow (< 1.5 Hz) Oscillations in the Rat Piriform (Olfactory) Cortex Are Functionally Correlated with Respiration. J. Neurosci. 2003; 23: 7993-8001.
59. Yanovsky Y, Ciatipis M, Draguhn A, Tort AB, Brankačk J. Slow oscillations in the mouse hippocampus entrained by nasal respiration. J. Neurosci. 2014; 34: 5949-5964.
60. Nguyen Chi V, Müller C, Wolfenstetter T, Yanovsky Y, Draguhn A, Tort AB, et al. Hippocampal Respiration-Driven Rhythm Distinct from Theta Oscillations in Awake Mice. J. Neurosci. 2016; 36: 162-177.
61. Ito J, Roy S, Liu Y, Cao Y, Fletcher M, Lu L, et al. Whisker barrel cortex delta oscillations and gamma power in the awake mouse are linked to respiration. Nat Commun. 2014; 5:3572, DOI: 10.1038/ncomms4572.
62. Tsanov M, Chah E, Reilly R, O'Mara SM. Respiratory cycle entrainment of septal neurons mediates the fast coupling of sniffing rate and hippocampal theta rhythm. Eur J Neurosci. 2014; 39: 957-974.
63. Lockmann AL, Laplagne DA, Leão RN, Tort ABA Respiration-Coupled Rhythm in the Rat Hippocampus Independent of Theta and Slow Oscillations. J Neurosci. 2016; 36: 5338-5352.
64. Zhong W, Ciatipis M, Wolfenstetter T, Jessberger J, Müller C, Ponsel S, et al. Selective entrainment of gamma subbands by different slow network oscillations. Proc. Natl Acad Sci U S A. 2017; 114: 4519-4524.
65. Biskamp J, Bartos M, Sauer JF. Organization of prefrontal network activity by respiration-related oscillations. Sci Rep. 2017; 7: 45508. doi: 10.1038/srep45508.
66. Lockmann ALV, Tort ABL. Nasal respiration entrains delta-frequency oscillations in the prefrontal cortex and hippocampus of rodents. Brain Struct Funct. 2018; 223: 1-3.
67. Moberly AH, Schreck M, Bhattarai JP, Zweifel LS, Luo W, Ma M. Olfactory inputs modulate respiration-related rhythmic activity in the prefrontal cortex and freezing behavior. Nat Commun. 2018; 9: 1528. doi: 10.1038/s41467-018-03988-1.
68. Piarulli A, Zaccaro A, Laurino M, Menicucci D, De Vito A, Bruschini L, et al. Ultra-slow mechanical stimulation of olfactory epithelium modulates consciousness by slowing cerebral rhythms in humans. Sci Rep. 2018; 26: 6581. doi: 10.1038/s41598-018-24924-9.
69. Perl O, Ravia A, Rubinson M, Eisen A, Soroka T, Mor N, et al., Human non-olfactory cognition phase-locked with inhalation. Nat Hum Behav. 2019; 3:501-512.
70. Kay LM, Beshel J, Brea J, Martin C, Rojas-Líbano D, Kopell N. Olfactory oscillations: the what, how and what for. Trends Neurosci. 2009; 32: 207-214.

71. Heck DH, Kozma R, Kay LM. The rhythm of memory: how breathing shapes memory function. J Neurophysiol. 2019; 122: 563-571.
72. Grosmaitre X, Santarelli LC, Tan J, Luo M, Ma M. Dual functions of mammalian olfactory sensory neurons as odor detectors and mechanical sensors. Nat Neurosci. 2007; 10: 348-354.
73. Ravel N, Pager J. Respiratory patterning of the rat olfactory bulb unit activity: nasal versus tracheal breathing. Neurosci Lett. 1990; 115:213-218.
74. Phillips ME, Sachdev RN, Willhite DC, Shepherd GM. Respiration drives network activity and modulates synaptic and circuit processing of lateral inhibition in the olfactory bulb. J. Neurosci. 2012; 32: 85-98.
75. Kleinfeld D, Deschênes M, Wang F, Moore JD. More than a rhythm of life: breathing as a binder of orofacial sensation. Nat Neurosci. 2014; 17:647-651.
76. Yackle K, Schwarz LA, Kam K, Sorokin JM, Huguenard JR, Feldman JL, et al. Breathing control center neurons that promote arousal in mice. Science. 2017; 355: 1411-1415.
77. Karalis N, Sirota A. Breathing coordinates limbic network dynamics underlying memory consolidation. BioRXiv. 2018; doi: https://doi.org/10.1101/392530.
78. McBride DW Jr, Hamill OP. Pressure-clamp technique for measurement of the relaxation kinetics of mechanosensitive channels. Trends Neurosci. 1993; 16:341-345. doi: 10.1016/0166-2236(93)90089-5. PMID: 7694402.
79. Maroto R, Kurosky A, Hamill OP. Mechanosensitive Ca(2+) permeant cation channels in human prostate tumor cells. Channels (Austin). 2012; 6:290-307. doi: 10.4161/chan.21063. Epub 2012 Jul 1. PMID: 22874798; PMCID: PMC3508908.
80. Lewis AH, Cui AF, McDonald MF, Grandl J. Transduction of Repetitive Mechanical Stimuli by Piezo1 and Piezo2 Ion Channels. Cell Rep. 2017; 20:19:2572-2585. doi: 10.1016/j.celrep.2017.05.079. PMID: 28636944; PMCID: PMC5646378.
81. Yasuma F, Hayano J. Respiratory sinus arrhythmia: why does the heartbeat synchronize with respiratory rhythm? Chest. 2004; 125: 683-690.
82. Mather M, Thayer J. How heart rate variability affects emotion regulation brain networks. Curr Opin Behav Sci. 2018; 19: 98-104.
83. Frysinger RC, Harper RM. Cardiac and respiratory correlations with unit discharge in human amygdala and hippocampus. Electroencephalogr Clin Neurophysiol. 1989; 72: 463-470.
84. Sobel N, PrabhakaranV, Hartley CA, Desmond JE, Zhao Z, Glover GH, et al. Odorant-Induced and Sniff-Induced Activation in the Cerebellum of the Human. J. Neurosc. 1998; 18: 8990-9001.
85. Cao Y, Liu Y, Jaeger D, Heck DH. Cerebellar Purkinje Cells Generate Highly Correlated Spontaneous Slow-Rate Fluctuations. Front Neural Circuits. 2017; 11(67); doi: 10.3389/fncir.2017.00067.
86. Vinje V, Ringstad G, Lindstrøm EK, Valnes LM, Rognes ME, Eide PK; et al. Respiratory influence on cerebrospinal fluid flow - a computational study based on long-term intracranial pressure measurements. Sci. Rep. 2019; 9: 9732. doi: 10.1038/s41598-019-46055-5.

87. Duvernoy HM, Delon S, Vannson JL. Cortical blood vessels of the human brain. Brain Res Bull. 1981: 7; 519-579. doi: 10.1016/0361-9230(81)90007-1. PMID: 7317796.
88. Heintz N (2004). Gene expression nervous system atlas (GENSAT). Nat Neurosci 2004; 7; 483.
89. Chesler AT, Szczot M, Bharucha-Goebel D, Čeko M, Donkervoort S, Laubacher C. et al The Role of PIEZO2 in Human Mechanosensation. N Engl J Med. 2016; 6; 1355-1364. doi: 10.1056/NEJMoa1602812. Epub 2016 Sep 21. PMID: 27653382; PMCID: PMC5911918.
90. Buzsaki G. Rhythms of the brain. 2006; Oxford: Oxford University Press.
91. Taberner FJ, Prato V, Schaefer I, Schrenk-Siemens K, Heppenstall PA, Lechner SG. Structure-guided examination of the mechanogating mechanism of PIEZO2. Proc Natl Acad Sci U S A. 2019; 116: 14260-69.
92. Wang L, Zhou H, Zhang M, Liu W, Deng T, Zhao Q, et al. Structure and mechanogating of the mammalian tactile channel PIEZO2. Nature. 2019; 573: 225-229.

Tables

Table 1. Antigenic peptides used to generate anti-PIEZO2 antibodies including the specific Ab staining of DRG and brain neuron in the neocortex (NC) hippocampus (HC) mitral cells of the olfactory bulb (MC/OB) and cerebellar Purkinje cells (PC). Human protein Atlas (HPA)

Ab	Antigenic peptide	DRG	Brain	Region/cell	Reference
1	C-termini 2440-2628	³90%	Yes	NC, HC, MC/OB, PC	Current
2	N-termini 351-485	<60%	N/T	-	17, 19
3	C-termini 2446-2568	N/T	Yes	NC, HC, PC	HPA
4	N-termini 845 -864	>90%	Yes	NC, HC	34
5	Internal 1091 -1104	>90%	Yes	NC, HC	34

Figures

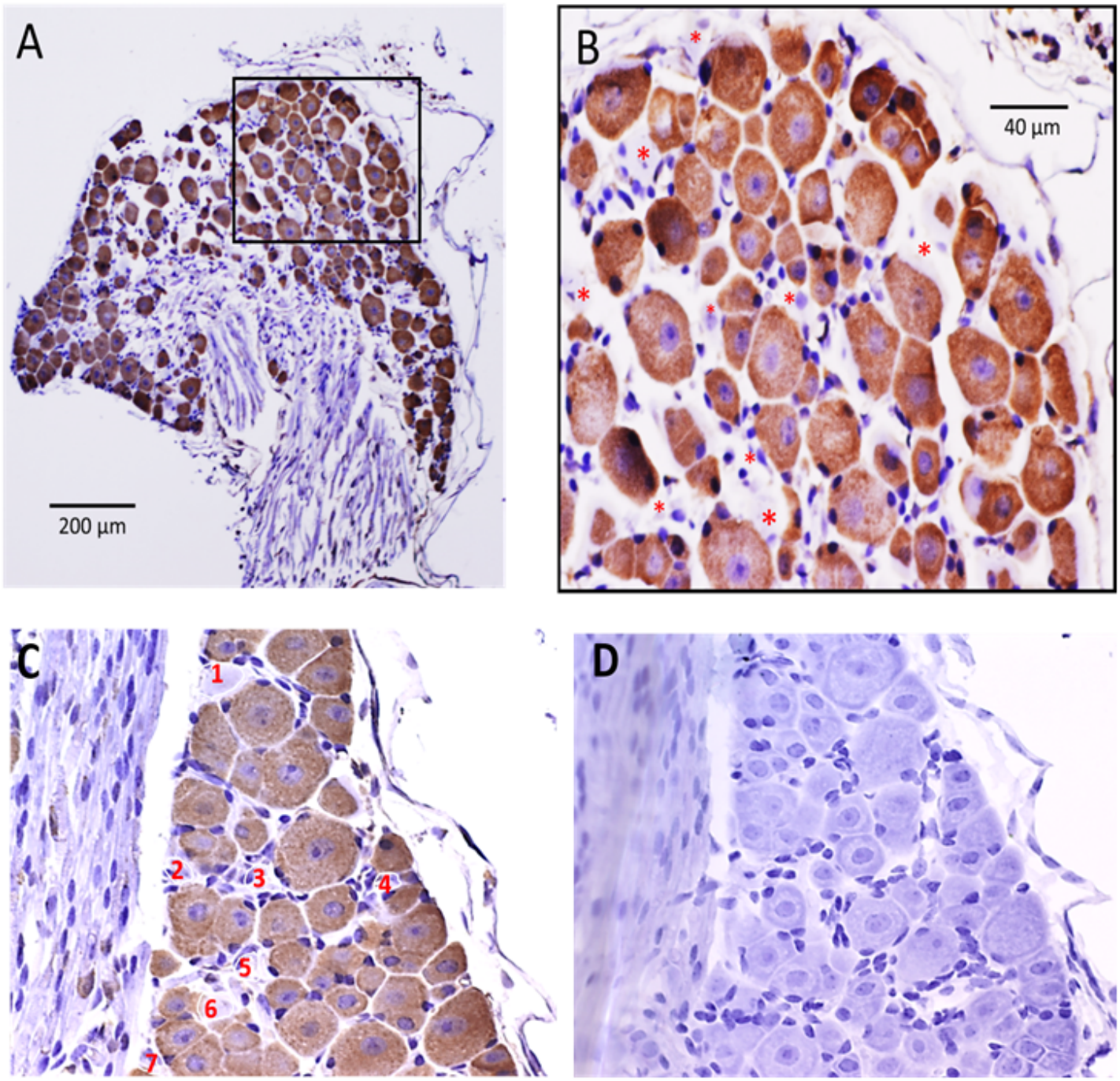

Figure 1

Immunohistochemical localization of Piezo2 in mouse DRG. A: The anti-Piezo2 Ab stained the majority of DRG neurons independent of soma size (range 10-50 µm in diameter). B: Higher magnification image of the section enclosed within the square in 1A shows that of the ~ 90 neurons present, only 9 neurons (i.e., indicated by red asterisks) showed no Ab staining and these appeared to be smaller diameter neurons. The numerous small blue structures (i.e., stained by the nuclear stain hematoxylin) around the perimeter of each neuron represent the cell bodies of satellite glia cells (SGCs) that includes their cell nucleus and very thin cytoplasmic processes that ensheath the neurons. The SGCs showed no Ab staining but this could be an issue of detection rather than a lack of Piezo2 expression. C: Another DRG slice from a

different mouse showing a similar pattern of staining most DRG neurons. D: The same slice treated with the same IHC protocol except without the anti-Piezo2 Ab present.

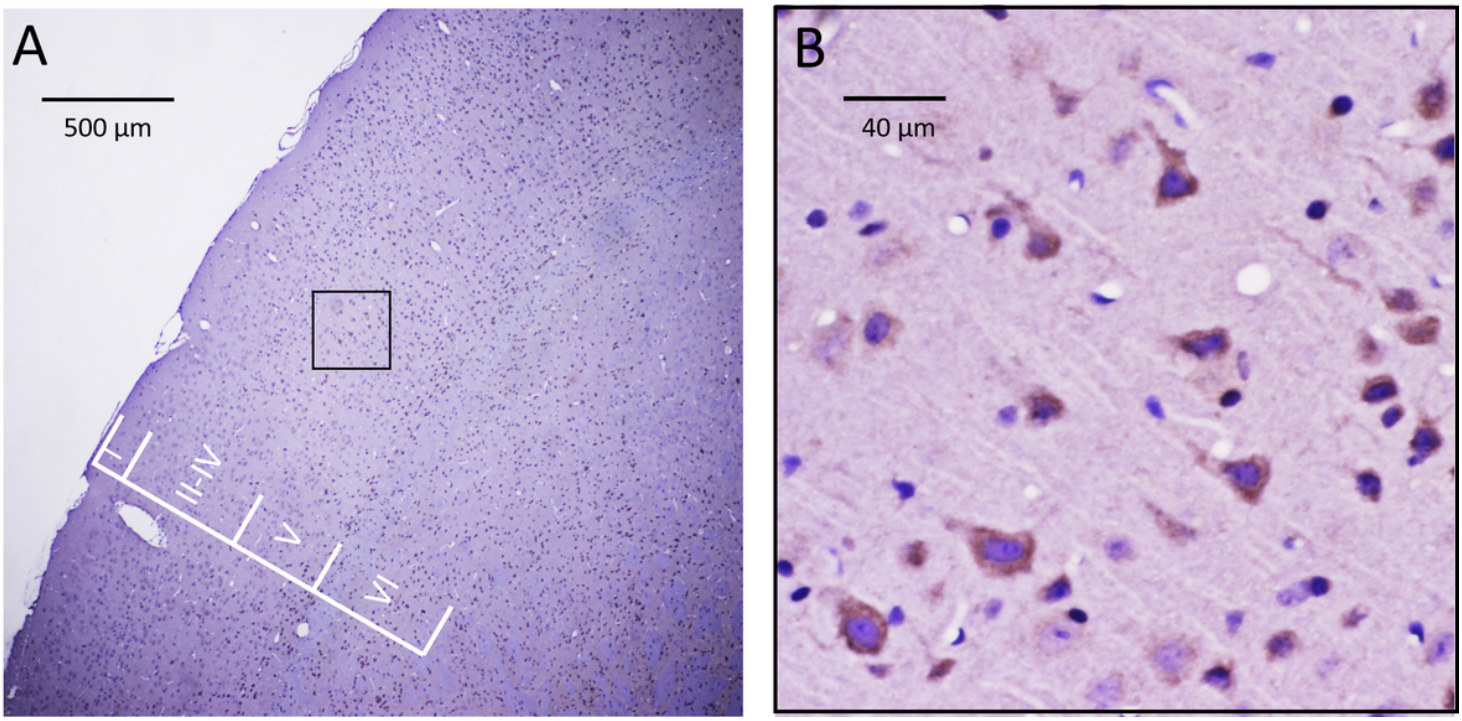

Figure 2

Immunohistochemical localization of Piezo2 in the mouse neocortex. A: The anti-Piezo2 Ab stained many cells throughout layers II-VI of the neocortex with minimal staining of cells in layer I. B: The selected region in A (i.e., within the black box) is shown at higher magnification and indicates the most commonly stained cells displayed a pyramidal shaped cell body with a thick process directed towards the pia (i.e., consistent with the apical dendrite of a pyramidal neuron). In contrast, there was no clear evidence of the staining of multipolar cells indicative of either stellate neurons or astrocytes.

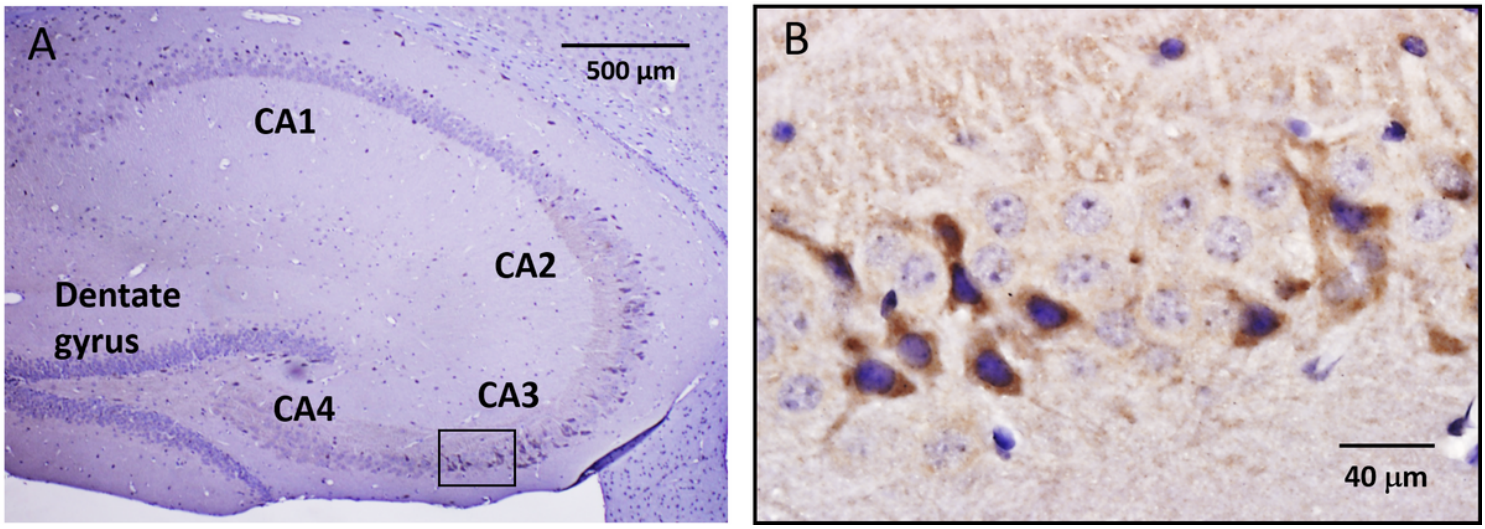

Figure 3

Immunohistochemical localization of Piezo2 in mouse hippocampus. A: Low magnification image of a hippocampal slice showing its distinct divisions that include the dentate gyrus (DG) and CA4-CA1 regions. B: The selected region in A (i.e., within the black box) that involves part of the CA3 region is shown at higher magnification and indicates at least 11 heavily stained cells which often displayed a pyramidal shaped cell body with a single prominent process. Within the same region, ~25 cells were stained blue by hematoxylin but showed no Ab staining. This all-or-none staining is at least consistent with idea of a stochastic on-off switch controlling Piezo2 expression.

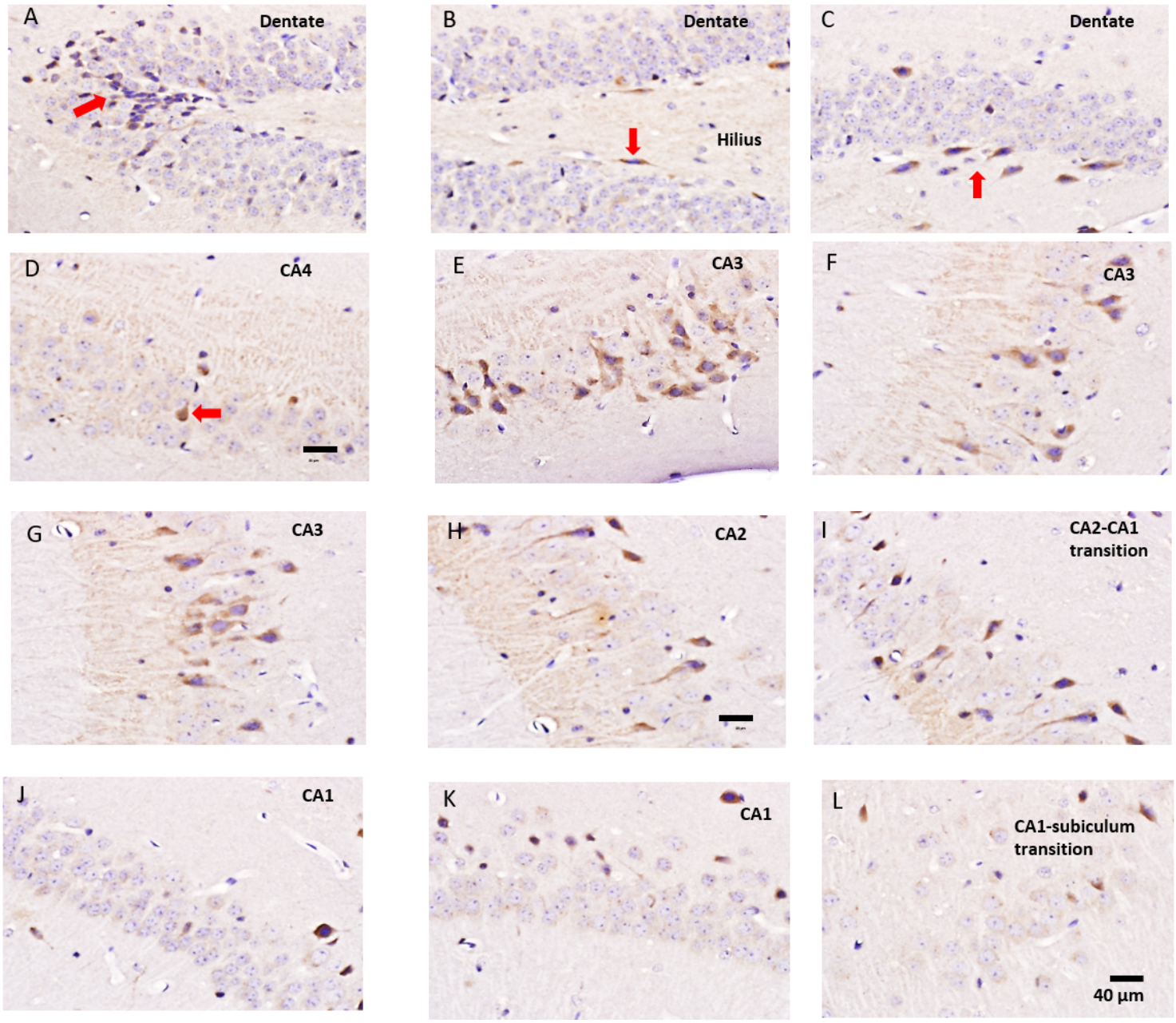

Figure 4

Ab staining of cells in different regions of the hippocampus. A: Shows the tip of the DG in which the majority of granule cells (i.e., round blue cells) are unstained by the Ab. However, a few cells at the very tip of the gyrus (red arrow) do show Ab staining. B: Shows the adjacent region of the DG in which 2-3 spindle

shaped cells (one indicated by red arrow) located in the subgranular zone show Ab staining. C: A continuing region further along the DG showing 7 spindle shaped cells stained by the anti-Piezo2 Ab. Over in the DG only 16 out of 1149 cells were stained by the Ab (i.e., 1.4%). D: Shows the hilius/C4 region with at least one darky-stained cell (red arrow) but with only 2 out of the 72 neurons clearly Ab stained. E-G: The CA3 region showing the highest density of Ab staining, with 50 out of 140 cells stained (36%) and displayed unitary thick processes (i.e., apical dendrites) consistent with pyramidal neurons. H: The CA2 region showing a somewhat lower density of stained neurons with 15 out of 71 cells stained (22%). I: A region near the CA2-CA1 transition that displays a further reduced density of stained neuron (23/305, i.e., ~ 8%) . J-K: CA1 regions showing even fewer clearly stained neurons. L: CA1 region transitioning into the subiculum that displayed no Ab-stained cells.

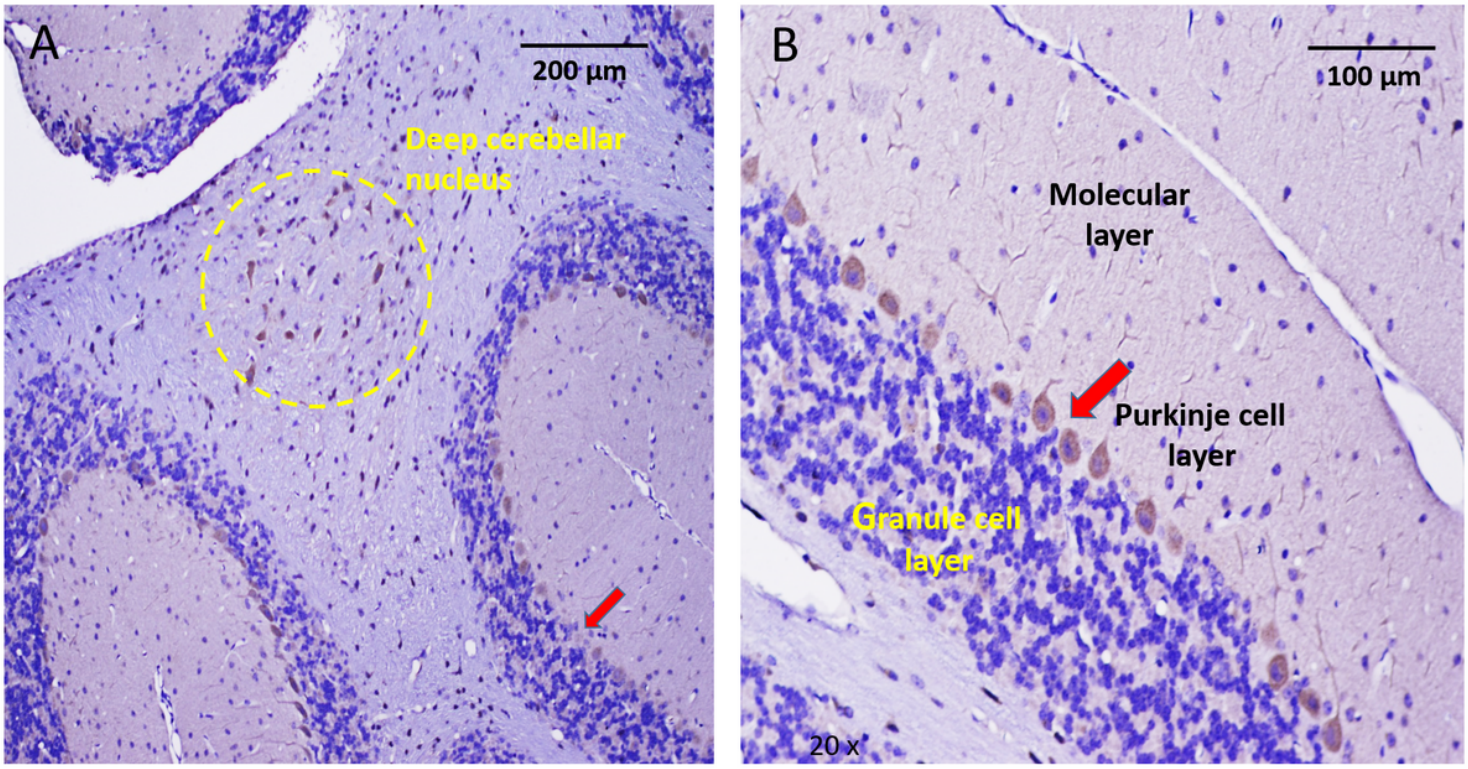

Figure 5

Immunohistochemical localization of Piezo2 in the cerebellum. A: Low magnification of a cerebellar slice indicating the stained Purkinje cell layer (red arrow) that separates the granule and molecular cell layers. The yellow dashed circle located within cerebellar white matter (arbor vitae) encloses a group of stained neurons presumably part of a deep cerebellar nucleus. B: Higher magnification of the cerebellar cortex showing the characteristic single layer of Purkinje cells which appear uniformly stained by the anti-Piezo2 Ab. In contrast to the stained Purkinje cells, the more numerous granular cells located within the granular cell layer were not stained. Similarly, apart from Purkinje cell dendrites there was no pronounced Ab staining of cells within the molecular layer.

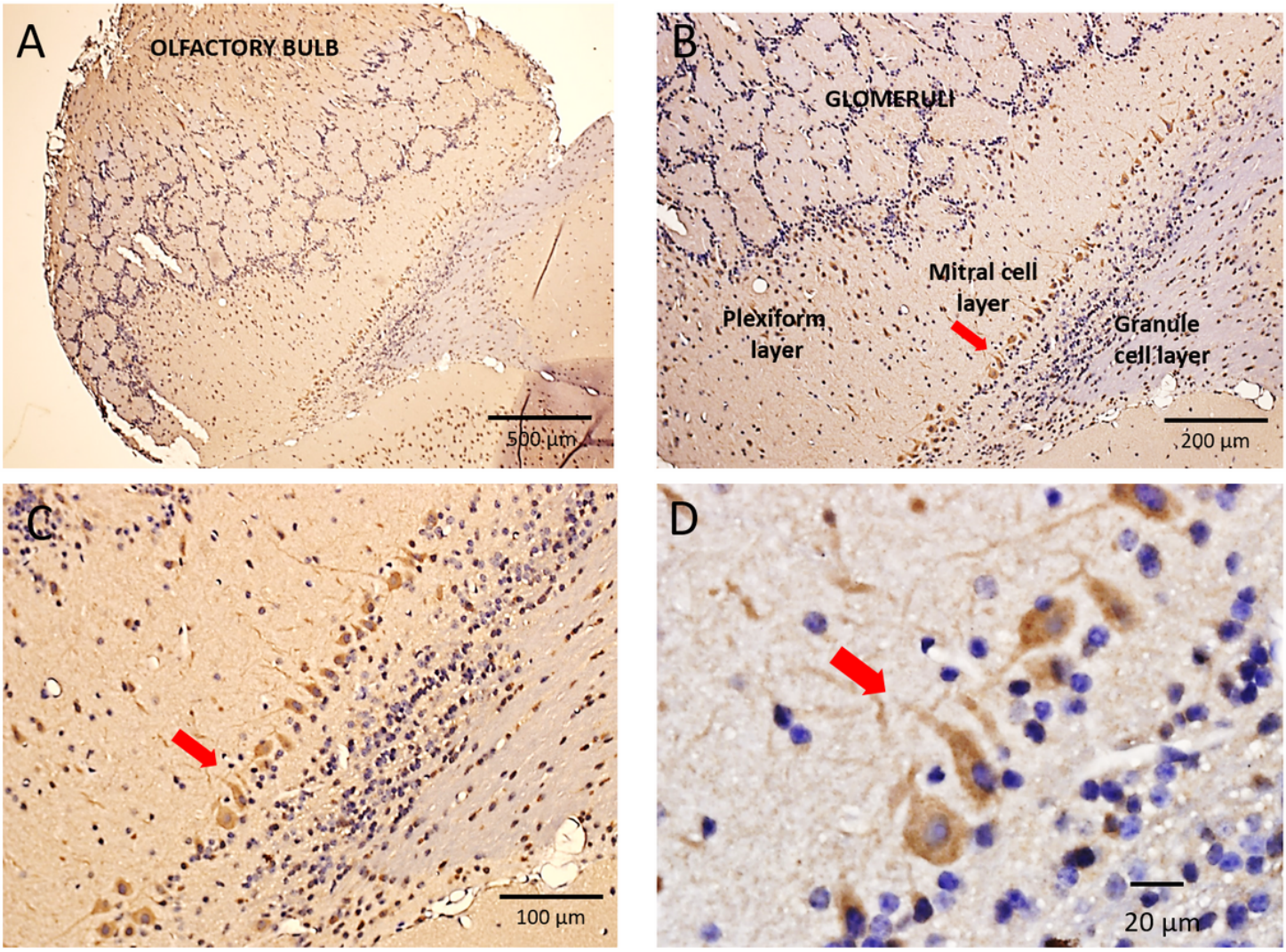

Figure 6

Immunohistochemical localization of Piezo2 in the mouse olfactory bulb. A: Shows a low magnification image of the mouse olfactory bulb (OB) with its characteristic circular/spherical glomeruli structures spanning the OB. These glomeruli include the synaptic connections formed between primary olfactory nerve (PON) axons and mitral cell dendrites. B-C: Higher magnification images (10x and 20x objectives) of the same slice showing the uniformly stained layer of mitral cell bodies (red arrows) that separate the external plexiform layer from the internal plexiform and granule cell layers. The mitral cells represent the major projection neuron of the OB and project their axons to the piriform and entorhinal cortices as well as the amygdala. The external plexiform layer includes the primary and lateral dendrites of the mitral cells that extend into and throughout the plexiform layer to reach the glomeruli. Also within this layer are the cell bodies and dendrites of the tufted cells, which did not appear stained. D: A still higher magnified image (60x objective) showing the morphology and staining of the mitral cells bodies and dendrites as well as the absence of staining of granule cells and the tufted cells in the granule cell and external plexiform layers, respectively.

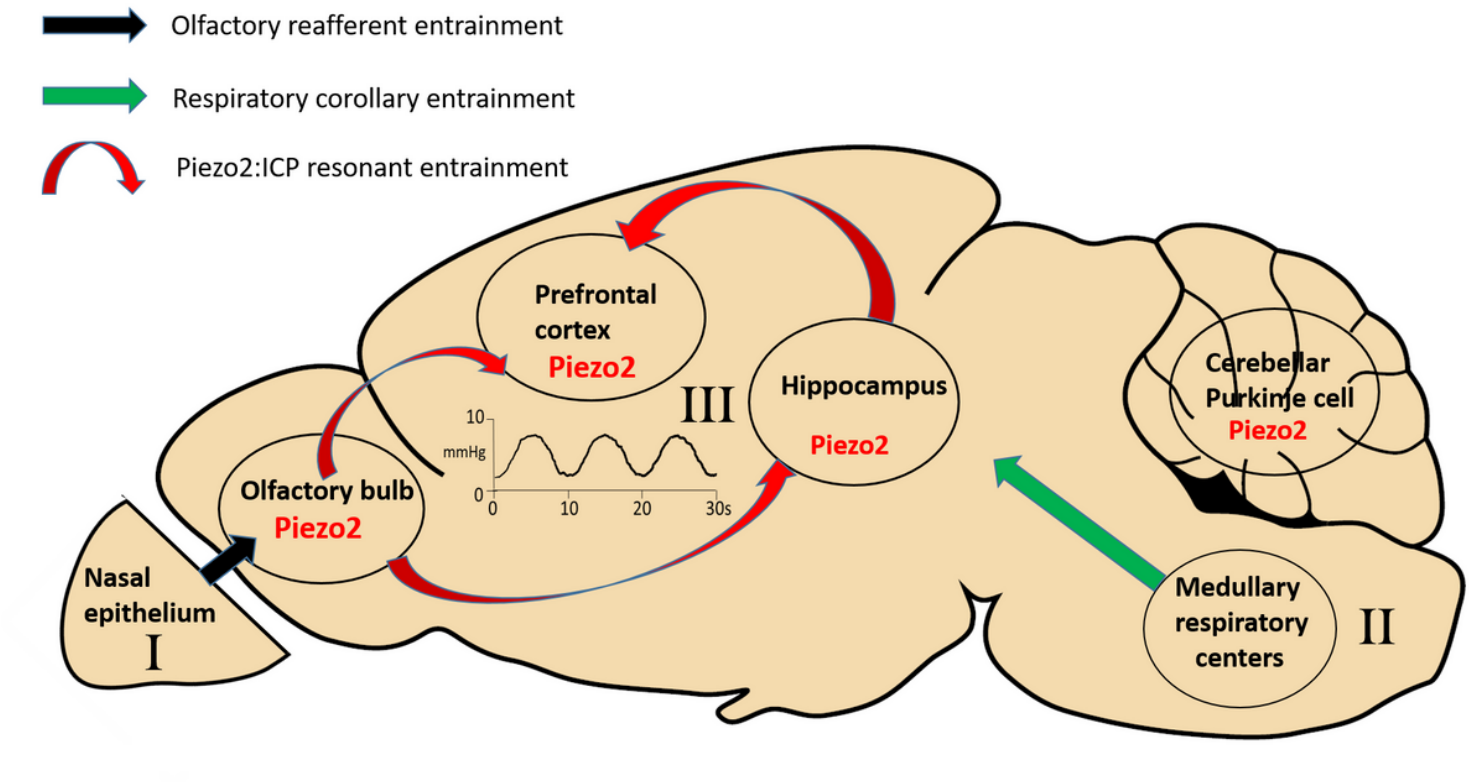

Figure 7

Mechanisms for respiration-induced entrainment of neural networks in widely spaced regions of the brain, The first mechanism involves respiratory olfactory re-afferent discharge (ORD) and originates in the nasal epithelium where primary olfactory neurons (PONs) which express olfactory G protein coupled receptors that are also mechanosensitive are able to detect the nasal airflow pressure changes associated with nasal breathing. The PONs through their direct synaptic connections (black arrow) with mitral cells and tufted cells in the OB cause respiratory entrainment of the neural activity within the OB. In turn, the OB entrains neural activity in the hippocampus and prefrontal cortex through their monosynaptic and/or polysynaptic connections (not shown) with these brain regions. The second mechanism, depends upon respiratory corollary discharge (RCD) arising from the neurons in the medullary respiratory nuclei that control the diaphragm muscles but also send efferent copy discharges to high brain regions (e.g., hippocampus and neocortex) via yet to be identified synaptic pathways. The third mechanism, intrinsic resonance discharge (IRD) depends upon the pressure sensitive channel, Piezo2, expressed in mitral cells of the OB and pyramidal cells of the hippocampus and neocortex. Piezo2, based on its demonstrated high sensitivity to low pressure pulses (≤, is proposed to transduce the ICP pulse associated with the respiratory cycle, thereby providing a synchronizing clock for brain activity. Finally, Piezo2 expression shown in cerebellar Purkinje cells, may explain the sniffing dependent activation of the PC in the human cerebellum.